

Provided for non-commercial research and education use.  
Not for reproduction, distribution or commercial use.



This article appeared in a journal published by Elsevier. The attached copy is furnished to the author for internal non-commercial research and education use, including for instruction at the authors institution and sharing with colleagues.

Other uses, including reproduction and distribution, or selling or licensing copies, or posting to personal, institutional or third party websites are prohibited.

In most cases authors are permitted to post their version of the article (e.g. in Word or Tex form) to their personal website or institutional repository. Authors requiring further information regarding Elsevier's archiving and manuscript policies are encouraged to visit:

<http://www.elsevier.com/copyright>



## Evolution of the one-phonon $2_{1,ms}^+$ mixed-symmetry state in $N = 80$ isotones as a local measure for the proton–neutron quadrupole interaction

T. Ahn<sup>a,b,c,\*</sup>, L. Coquard<sup>c</sup>, N. Pietralla<sup>c</sup>, G. Rainovski<sup>d</sup>, A. Costin<sup>b</sup>, R.V.F. Janssens<sup>e</sup>, C.J. Lister<sup>e</sup>, M. Carpenter<sup>e</sup>, S. Zhu<sup>e</sup>, K. Heyde<sup>f</sup>

<sup>a</sup> Wright Nuclear Structure Laboratory, Yale University, New Haven, CT 06520, USA

<sup>b</sup> Department of Physics and Astronomy, Stony Brook University, Stony Brook, NY 11794-3800, USA

<sup>c</sup> Institut für Kernphysik, Technische Universität Darmstadt, 64289, Darmstadt, Germany

<sup>d</sup> Faculty of Physics, St. Kliment Ohridski University of Sofia, Sofia 1164, Bulgaria

<sup>e</sup> Argonne National Laboratory, 700 South Cass Avenue, Argonne, IL 60439, USA

<sup>f</sup> Department of Subatomic and Radiation Physics, Proeftuinstraat, 86 B-9000 Ghent, Belgium

### ARTICLE INFO

#### Article history:

Received 11 December 2008

Received in revised form 8 May 2009

Accepted 30 June 2009

Available online 4 July 2009

Editor: V. Metag

#### PACS:

21.10.Re

23.20.Gq

25.70.De

27.60.+j

#### Keywords:

Mixed-symmetry states

Coulomb excitation

Angular distribution

Proton–neutron quadrupole interaction

### ABSTRACT

An inverse kinematics Coulomb excitation experiment was performed to obtain absolute  $E2$  and  $M1$  transition strengths in  $^{134}\text{Xe}$ . The measured transition strengths indicate that the  $2_3^+$  state of  $^{134}\text{Xe}$  is the dominant fragment of the one-phonon  $2_{1,ms}^+$  mixed-symmetry state. Comparing the energy of the  $2_{1,ms}^+$  mixed-symmetry state in  $^{134}\text{Xe}$  to that of the  $2_{1,ms}^+$  levels in the  $N = 80$  isotonic chain indicates that the separation in energy between the fully-symmetric  $2_1^+$  state and the  $2_{1,ms}^+$  level increases as a function of the number of proton pairs outside the  $Z = 50$  shell closure. This behavior can be understood as resulting from the mixing of the basic components of a two-fluid quantum system. A phenomenological fit based on this concept was performed. It provides the first experimental estimate of the strength of the proton–neutron quadrupole interaction derived from nuclear collective states with symmetric and antisymmetric nature.

© 2009 Elsevier B.V. All rights reserved.

The evolution of nuclear collectivity depends critically on the proton–neutron interaction in the valence shell. This fact is evident from the scaling of collective observables, such as the  $E2$  excitation strength of the  $2_1^+$  state of even–even nuclei, with the product of valence nucleon numbers,  $N_p N_n$  [1]. Despite its fundamental role, measurements of the size of the proton–neutron interaction in the valence shell [2] are rare and indirect. This is because the  $N_p N_n$  dependence was studied mostly for the low-lying collective states whose properties are experimentally known best. In the framework of the interacting boson model [3], these states are described by boson wave functions that are symmetric with respect to the pairwise exchange of proton–neutron boson labels quantified by a maximum  $F$ -spin quantum number. Proton–neutron symmetric

states are insensitive to certain parts of the proton–neutron interaction, e.g., to the Majorana term in the Interacting Boson Model-2 (IBM-2) Hamiltonian, and information on the proton–neutron interaction requires systematic studies over a specific nuclear region.

It has previously been pointed out [4] that local information on the proton–neutron quadrupole interaction in the valence shell can be deduced from the separation between symmetric and so-called mixed-symmetry states (MSSs) [5]. However, due to the lack of experimental data this expectation is still lacking verification.

Mixed-symmetry states are defined in the IBM-2 [3] and constitute a class of collective states that contain anti-symmetric parts with respect to the pairwise exchange of proton and neutron bosons. This symmetry between the two types of bosons can be quantified by the  $F$  spin [6], which is analogous to the concept of isospin for nucleons. Vibrational nuclei exhibit a one-quadrupole phonon excitation as the lowest state of mixed proton–neutron symmetry. This  $2_{1,ms}^+$  state has the  $F$  spin quantum number  $F = F_{\max} - 1$ , where  $F_{\max}$  is the maximal value of  $F$ . The unique sig-

\* Corresponding author at: Wright Nuclear Structure Laboratory, Yale University, New Haven, CT 06520, USA.

E-mail address: tan.ahn@yale.edu (T. Ahn).

nature for MSSs is the occurrence of strong M1 transitions to low-energy symmetric collective states. The evolution of the  $2^+_{1,ms}$  state in vibrational nuclei can provide direct information on the strength of the local proton–neutron quadrupole interaction in the valence shell [4].

A number of mixed-symmetry states have been identified in the mass  $A = 140$  region [7–14]. A review of the experimental status for multi-phonon states with mixed proton–neutron symmetry is given in Ref. [15]. Among these are the ones found in  $^{136}\text{Ba}$  [8] and  $^{138}\text{Ce}$  [9], both of which are  $N = 80$  isotones. The latter experiment gave evidence for the concept of shell stabilization of single, isolated MSSs [9], predicting the existence of comparable, unperturbed MSSs in vibrational nuclei away from sub-shell closures. Using this concept, a well-developed  $2^+_{1,ms}$  state should be expected in the  $N = 80$  isotope  $^{134}\text{Xe}$ , as this is a nucleus with four valence protons filling half of the  $\pi 1g_{7/2}$  sub-shell. Therefore, an experiment was carried out to investigate the one-phonon  $2^+_{1,ms}$  state of  $^{134}\text{Xe}$  by measuring absolute electromagnetic transition strengths using the method of Coulomb excitation with inverse kinematics. Furthermore, knowledge about the properties of the  $2^+_{1,ms}$  state of  $^{134}\text{Xe}$  should shed light on the evolution of these states in the  $N = 80$  isotonic chain towards the  $Z = 50$  proton shell closure. As we will demonstrate below, that information allows for the extraction of the local proton–neutron quadrupole interaction from the properties of both symmetric and MSSs [4].

An inverse kinematics Coulomb excitation experiment was carried out at Argonne National Laboratory using a  $^{134}\text{Xe}$  beam impinging on a natural carbon target with an effective thickness of  $1.2 \text{ mg/cm}^2$ . The reaction  $^{12}\text{C}(^{134}\text{Xe}, ^{134}\text{Xe}^*)$  was studied. The beam was provided by the superconducting ATLAS linear accelerator with an energy of 435 MeV, which corresponds to 82% of the Coulomb barrier. The beam had an intensity of approximately 1 pA. Emitted  $\gamma$ -rays from the reaction were detected with the Gammasphere array [16,17], which consisted of 101 Compton-suppressed, high-purity germanium detectors. The condition defining an event was a 1-fold or higher prompt multiplicity. The experiment ran for approximately 38 hours and a total of  $8.4 \times 10^8$  events were recorded. In the offline analysis, the time spectra were used to select prompt  $\gamma$ -rays corresponding to the beam pulses hitting the target. Time gates on the background were also used to subtract peaks from room background. A Doppler-corrected and background-subtracted energy spectrum for the sum of all detectors in Gammasphere is provided in Fig. 1. Four new  $\gamma$ -ray transitions were observed. Though the area of the 847-keV peak, which corresponds to the intensity of the  $2^+_1 \rightarrow 0^+_1$  transition, is a few orders of magnitude larger than the transition intensities from the higher-lying states, the peaks for these transitions can clearly be seen in the higher energy part of the spectrum. A low- $Z$  target and a beam energy about 20% below the Coulomb barrier were chosen to maximize contributions from one-step excitations.

A total of  $2.6 \times 10^6$  events with multiplicity 2 and higher were sorted into a  $E_\gamma$ - $E_\gamma$  coincidence matrix, where the  $\gamma$ -ray energies were corrected for Doppler shifts. The subsequent coincidence analysis of this matrix was used to verify the low-energy level scheme of  $^{134}\text{Xe}$  and to identify weak  $\gamma$ -ray transitions. Two out of the four newly observed  $\gamma$ -ray transitions were placed in the level scheme from the analysis. All transitions observed in the experiment are shown in Fig. 2. A 921-keV  $\gamma$ -ray was determined to be in coincidence with the 847-keV and 1100-keV transitions which suggests that the 921-keV transition is connecting the 2867-keV and 1947-keV states. The second new transition is the 1254-keV  $\gamma$ -ray connecting the 2867-keV and 1614-keV levels. It is close in energy to the 1269-keV transition and both peaks overlap in the observed singles spectrum, as can be seen in Fig. 1, but it can be inferred from the relatively large peak width that it corresponds to a doublet. Furthermore, by gating on the 767-keV or 1614-keV transition, the 1254-keV peak can be clearly isolated in the coincidence spectrum. It is possible that the 2867-keV level observed is the hitherto unobserved  $3^-_1$  state [18] due to the relatively strong

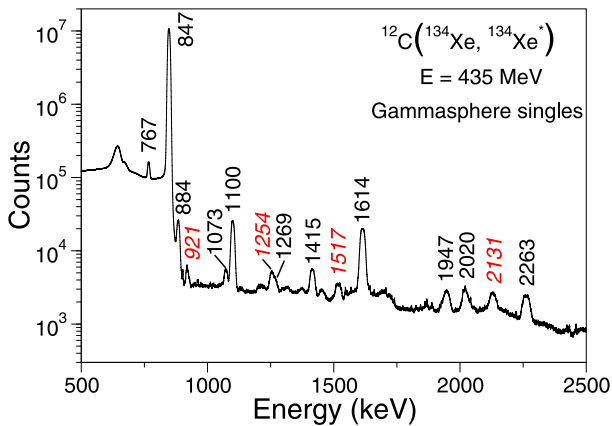


Fig. 1. Doppler-corrected and background-subtracted  $\gamma$ -ray spectrum for the sum of all detectors in Gammasphere. New  $\gamma$ -ray transitions are indicated in oblique type.

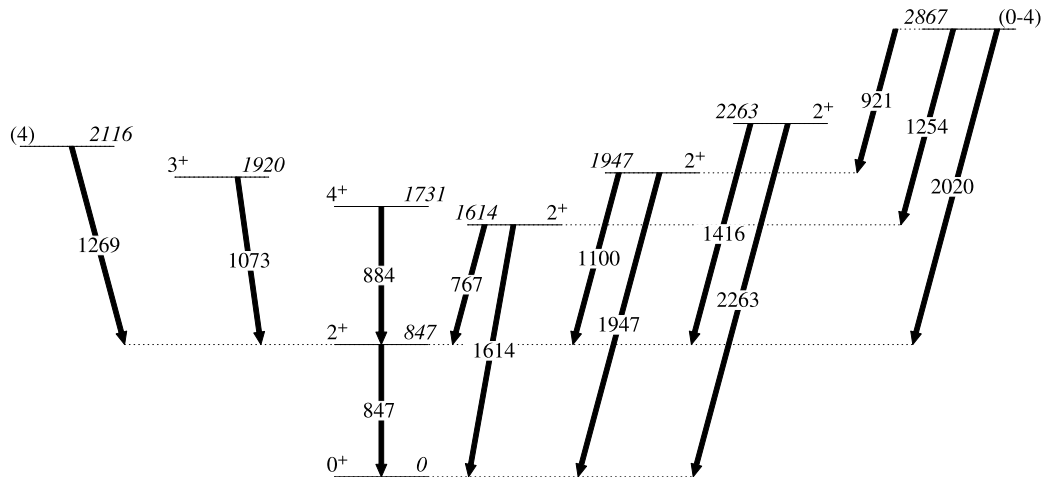


Fig. 2. A level scheme of  $^{134}\text{Xe}$ . The transitions observed in the experiment and their corresponding levels are shown.

**Table 1**

Energy of the state  $E_{\text{level}}$ , spin and parity  $J^\pi$ , lifetime  $\tau$ , energy of the  $\gamma$ -ray transition  $E_\gamma$ , spin and parity of the final state  $J^\pi_{\text{final}}$ , relative  $\gamma$ -ray intensity  $I_\gamma$ , normalized angular distribution coefficients  $A_2/A_0$  and  $A_4/A_0$ , multipole mixing ratio  $\delta$ , and transition strengths  $B(E2)$  and  $B(M1)$  for all transitions in  $^{134}\text{Xe}$  measured in the present work.

$E_{\text{level}}$ (keV)	$J^\pi$	$\tau$ (ps)	$E_\gamma$ (keV)	$J^\pi_{\text{final}}$	$I_\gamma$	$A_2/A_0$	$A_4/A_0$	$\delta$	$B(E2)$ (W.u.)	$B(M1)$ ( $\mu_N^2$ )
847	$2_1^+$	3.0(2) <sup>a</sup>	847	$0_1^+$	1000(9)	0.119(7)	-0.006(9)		15.3(11) <sup>a</sup>	
1614	$2_2^+$	1.9(1)	767	$2_1^+$	4.70(5)	-0.262(8)	-0.01(1)	-1.5(2)	20(2)	0.015(1)
			1614	$0_1^+$	4.93(8)	0.28(1)	-0.06(2)		0.74(5)	
1731	$4_1^+$	3.2(2) <sup>a</sup>	884	$2_1^+$	1.79(2)				11.6(8) <sup>a</sup>	
1920	$3_1^+$		1073	$2_1^+$	0.355(5)			0.16(2) <sup>a</sup>		
1947	$2_3^+$	0.23(2)	1100	$2_1^+$	3.44(4)	0.27(1)	0.01(1)	0.08(2)	0.56(4)	0.30(2)
			1947	$0_1^+$	0.515(9)	0.306 <sup>b</sup>	-0.074 <sup>b</sup>		0.72(7)	
2116	(4)		1269	$2_1^+$						
2263	$2_4^+$	0.54(4)	1415	$2_1^+$	0.73(1)	0.33(2)	0.07(2)	0.14(2)	0.14(1) <sup>c</sup>	0.041(3) <sup>c</sup>
								1.6(1)	5.6(4) <sup>d</sup>	0.012(1) <sup>d</sup>
2867	(0-4)		921	$2_3^+$	0.25(4)					
			1254	$2_2^+$	0.35(6)					
			2020	$2_1^+$	0.38(6)					

<sup>a</sup> Value from Ref. [19].

<sup>b</sup> Calculated from theory of Coulomb excitation.

<sup>c</sup> Derived using value of  $\delta = 0.14(2)$ .

<sup>d</sup> Derived using value of  $\delta = 1.6(1)$ .

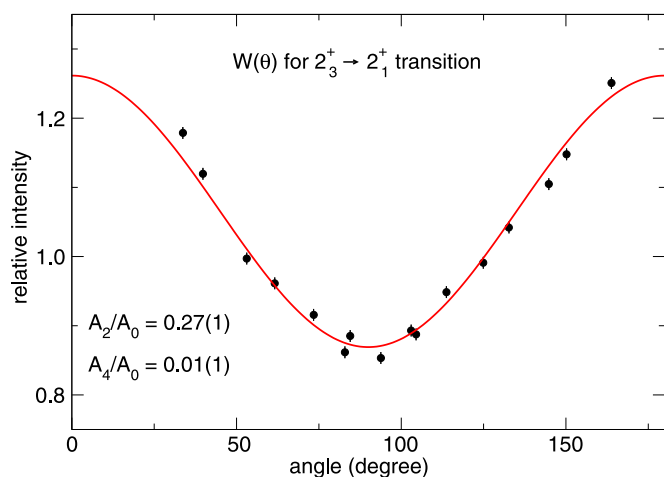


**Fig. 3.** Measured angular distribution for the  $2_3^+ \rightarrow 2_1^+$  transition along with the best fit curve using the calculated values for the statistical tensors for this state. A corresponding value of  $\delta = 0.08(2)$  was obtained.

states found in the neighboring even-even Xe isotopes, namely the 2469-keV state in  $^{132}\text{Xe}$  and the 3275-keV level in  $^{136}\text{Xe}$  [18]. The spectroscopic information for all the levels and transitions observed in the present experiment is summarized in Table 1.

The spins of the levels were assigned on the basis of an angular distribution analysis [20]. The intensities of the  $\gamma$ -rays were measured over the 16 rings of Gammasphere, corrected for the Lorentz boost [21] and fitted with the angular distribution function [20]. The data and the fitted curve for the  $2_3^+ \rightarrow 2_1^+$  transition are presented in Fig. 3. The experimental  $A_2/A_0$  and  $A_4/A_0$  coefficients for the  $2^+ \rightarrow 0^+$  transitions, which have a pure  $E2$  multipolarity, can unambiguously determine the orientation of the  $2^+$  states, which is quantified by statistical tensors [20]. The statistical tensors of the  $2^+$  states can then be used to determine the multipole mixing ratios for the mixed transitions between excited  $2^+$  states. Unfortunately, this procedure for determination of the multipole mixing ratio was applicable only for the  $2_2^+ \rightarrow 2_1^+$  transition. For the  $2_3^+ \rightarrow 0_1^+$  and  $2_4^+ \rightarrow 0_1^+$  transitions, a precise fit for the an-

gular distribution coefficients, and hence the  $2^+$  state orientations, could not be made due to background contamination. This contamination is possibly from fusion reactions, which result from carbon ions scattering from the target and hitting the target chamber. The ions scattered in the forward angles would have sufficient energy for this to happen. The  $\gamma$  rays resulting from the fusion reaction are then correlated with the beam pulses. Such background cannot be subtracted using time gates alone as there is no way to differentiate in time between good events and beam-related background events. Since angular distributions could not be measured for the  $2_3^+ \rightarrow 0_1^+$  and  $2_4^+ \rightarrow 0_1^+$  transitions, the statistical tensors of the  $2_3^+$  and  $2_4^+$  states were calculated from the semi-classical theory of Coulomb excitation using first-order perturbation theory as outlined in Ref. [22] and the multiple step Coulomb excitation program CLX [23,24], based on the program by Winther and de Boer [25]. The calculations were done for a beam energy of 435 MeV. For the calculation using the semi-classical theory, it assumes that the states were populated with direct, one-step Coulomb excitation without any second order effects. The second calculation for the statistical tensors was done using CLX, which is not restricted to one-step excitations. To verify using the calculated statistical tensors for the  $2_3^+$  and  $2_4^+$  states, we have calculated the statistical tensors for the  $2_2^+$  state using both methods mentioned above. The resulting statistical tensors were within the uncertainties of the ones determined experimentally from the measured angular distribution of the  $2_2^+ \rightarrow 0_1^+$   $\gamma$  ray. This shows that two-step processes are not significant for determining the orientation of the two-phonon  $2_2^+$  state and the same should be true for the  $2_3^+$  and  $2_4^+$  states. Therefore, the statistical tensors for the  $2_3^+$  and  $2_4^+$  states should be well described by their calculated values. For the  $2_4^+ \rightarrow 2_1^+$  transition, two possible values of  $\delta$  were deduced. The small range of possible values for  $A_4/A_0$ , and the limited precision achieved in measuring them, lead to this ambiguity. In either case, the  $B(M1; 2_4^+ \rightarrow 2_1^+)$  value is below 0.05  $\mu_N^2$ . For the  $2_3^+ \rightarrow 2_1^+$  transition the  $E2/M1$  multipole mixing ratio  $\delta = 0.08(2)$  is favored by our value of  $A_4/A_0$  by about three standard deviations (compare with Fig. 2d of Ref. [9]). Furthermore, the less likely alternative  $\delta = 1.86(5)$  leads to a value for the

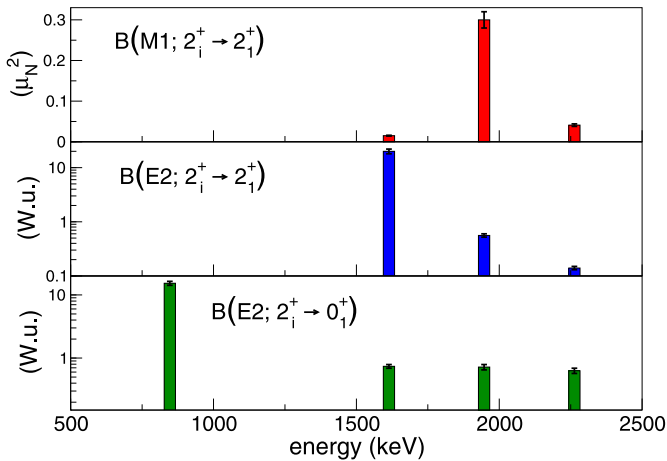


**Fig. 4.** The values for  $B(M1; 2_1^+ \rightarrow 2_1^+)$ ,  $B(E2; 2_1^+ \rightarrow 2_1^+)$ , and  $B(E2; 2_1^+ \rightarrow 0_1^+)$  strengths deduced in the present measurement are shown on the top, middle, and bottom plots, respectively. The transitions from the  $2_4^+$  state were deduced using the smaller values of  $\delta$ . See text for details.

$B(E2; 2_3^+ \rightarrow 2_1^+) = 57(5)$  W.u., which is unreasonably large for an E2 transition forbidden by phonon selection rules for vibrational nuclei. We adopt the value  $\delta = 0.08(2)$  as shown in Table 1. The convention of Krane, Steffen, and Wheeler [26,27] was used for the multipole mixing ratios.

The relative population of all the states excited in the Coulomb excitation experiment was deduced from the total  $\gamma$ -ray transition intensities. The relative  $\gamma$ -ray yields with respect to the  $2_1^+$  state measure the relative Coulomb excitation cross-sections. These data were fit with the multiple-step Coulomb excitation program CLX to determine transition matrix elements. This was done by finding the values of the input matrix elements which best reproduce the relative populations of all the states measured in the experiment. Branching ratios, multipole mixing ratios and the known value of the  $B(E2; 2_1^+ \rightarrow 0_1^+)$  transition probability [19] were used to constrain the number of independent matrix elements involved in the decay or excitation of a specific state. An assumption was made where the electric quadrupole moments have been set to zero, since their contribution to Coulomb excitation cross sections is a second order effect and should be small for spherical nuclei and for Coulomb excitation reactions with a light-ion reaction partner. The CLX program uses the RPT phase convention [28], which results in the matrix elements taking on real values. In the program input, there is an ambiguity in the phase of the matrix element, which can either be +1 or -1. This may affect the final values of the matrix elements, but it was not feasible to try all possible phase combinations for the given set of matrix elements. It is assumed that, for the case of  $^{134}\text{Xe}$ , which is close to being a spherical nucleus, the phase of the matrix elements will only affect the final transition strengths within the magnitude of the uncertainties. The absolute M1 transition strengths for transitions of mixed multipolarity were obtained from the measured values of the transitions' multipole mixing ratios. All of the determined transition strengths are tabulated in Table 1. It should be noted that for the transitions from the  $2_4^+$  state, due to the ambiguity in the value for  $\delta$  discussed above, two different sets of transition strengths were deduced. The transition strength obtained for the smaller values of  $\delta$  is plotted in Fig. 4. The resulting ground state transition strength for the  $2_4^+$  state depends slightly on the choice of the multipole mixing ratio for the  $2_4^+ \rightarrow 2_1^+$  transition because of a possible two-step contribution to the total Coulomb excitation cross section. This effect is, however smaller than the given error bars and is neglected.

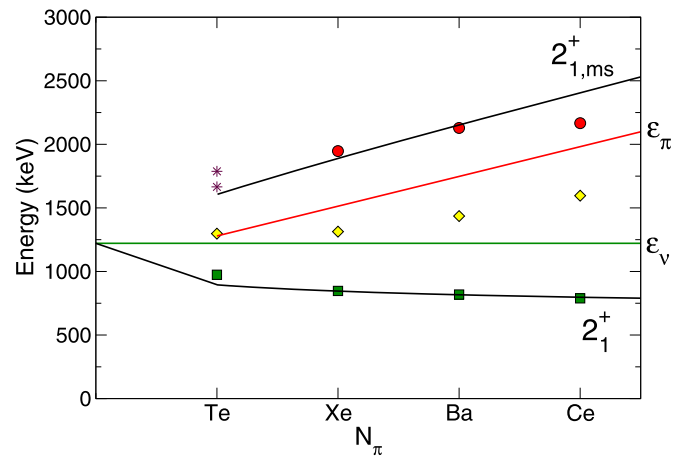


**Fig. 5.** Fit of the experimental energies of the  $2_{1,ms}^+$  and  $2_1^+$  levels in the  $N = 80$  isotones shown as filled circles and squares, respectively. The lines labeled  $\epsilon_\pi$  and  $\epsilon_\nu$  represent the unperturbed energy of the proton and neutron state, respectively. The energies of the  $2_1^+$  states in the corresponding  $N = 82$  isotones are given as diamonds. Tentative  $2_1^+$  states in  $^{132}\text{Te}$  are shown as asterisks.

From the distribution of M1 strengths, the  $2_3^+$  state can unambiguously be identified as the main fragment of the  $2_{1,ms}^+$  state as its  $B(M1)$  value dominates the  $2^+ \rightarrow 2_1^+$  M1 strength distribution plotted in Fig. 4. Though there is an ambiguity in the M1 transition strength for the  $2_4^+$  state, both possible values are small compared to that of the  $2_3^+$  state. The large  $B(M1)$  value for the  $2_3^+$  state is in agreement with recent microscopic calculations by Lo Iudice et al. using the quasi-particle phonon model [29].

In the  $N = 80$  isotones, it is observed that the  $2_1^+$  state decreases in energy with the increasing number of proton pairs  $N_\pi$ . Here we define  $N_\pi = \frac{N_p}{2}$  where  $N_p$  is the number of protons outside the  $Z = 50$  shell closure. An analogous definition for the number of neutron hole pairs  $N_\nu$  outside the  $N = 82$  shell closure is used. Within the IBM-2, these pairs can be identified with the proton and neutron bosons, respectively. In contrast to the  $2_1^+$  state, the  $2_{1,ms}^+$  state increases in energy as one goes to larger values of  $N_\pi$  (see Fig. 5), thus the separation between the two levels becomes larger as a function of  $N_\pi N_\nu$ . According to the two-state mixing scheme outlined in Ref. [4], a fit was performed for the first time to the energy splitting of the observed  $2_1^+$  and  $2_{1,ms}^+$  states. In this scheme, the observed  $2_1^+$  and  $2_{1,ms}^+$  states arise through the mixing of the unperturbed proton and neutron  $2^+$  configurations in which the proton-neutron coupling matrix element increases as a function of the product  $N_\pi N_\nu$ . The interaction between the two states originates from the proton-neutron quadrupole interaction and, thus, it was parametrized as  $V(N_\pi) = \beta \sqrt{N_\pi N_\nu}$ , since the interaction scales to first order as  $\sqrt{N_\pi N_\nu}$  for low boson numbers and large degeneracies [4]. It is interesting to note that using the 2-level model which starts from unperturbed  $2_\pi^+$  proton and  $2_\nu^+$  neutron excitations and includes a residual quadrupole-quadrupole proton-neutron interaction, the atomic mass number dependence of the energy of the first excited  $2_1^+$  symmetric proton-neutron combination was derived using a seniority scheme [4]. This particular mass dependence gives rise to a specific expression for the  $\beta$  parameter in the  $V(N_\pi)$  expression defined above. The average energy of the observed  $2_1^+$  and  $2_{1,ms}^+$  states increases as a function of proton boson number, which for a constant value of  $N_\nu$  in an isotonic sequence requires an increase in the proton boson energy. Indeed, the  $2_1^+$  states in the neighboring semi-magic  $N = 82$  isotones increase in energy almost linearly with valence proton number, as can be seen in Fig. 5. Consequently, the un-



perturbed energy of the proton state was linearly parametrized by the expression  $\epsilon_\pi(N_\pi) = a + b(N_\pi - 1)$  as a first order approximation, where  $a$  was chosen to be equal to the energy of the  $2_1^+$  state in the neutron-closed shell nucleus  $^{134}\text{Te}$ . This is because we assume that the one-phonon excitation in this nucleus is due solely to the single proton pair outside of the  $Z = 50$  closed shell. Likewise, the value for  $\epsilon_\nu$  is taken to be constant for the  $N = 80$  isotones, and is set equal to the energy of the  $2_1^+$  state of  $^{130}\text{Sn}$  for the analogous reason that the one-phonon excitation is only due to the single neutron hole pair outside of the  $N = 82$  closed shell. The values of the parameters used were  $a = \epsilon_\pi(N_\pi = 1) = E_{2_1^+}(^{134}\text{Te}) = 1279$  keV,  $\epsilon_\nu = E_{2_1^+}(^{130}\text{Sn}) = 1221$  keV. The value of the parameters  $b$  and  $\beta$  were derived from a least-squares fit to the experimentally observed evolution of the energy of the one-phonon fully symmetric (the  $2_1^+$ ) state in the  $N = 80$  isotonic chain and the one-phonon MSS of  $^{134}\text{Xe}$  and  $^{136}\text{Ba}$  (see Fig. 5). The fit yielded the values  $b = 0.23(4)$  MeV, and  $\beta = 0.35(1)$  MeV. The data point for the  $2_{1,\text{ms}}^+$  state of  $^{138}\text{Ce}$  was not included in the fit because the lack of shell stabilization of mixed-symmetry structures at the  $Z = 58$  sub-shell closure [9] would have biased the numerical result for the fitted parameters.

A fit to the excitation energy of the  $2_1^+$  state in the even-even Te, Xe, Ba, Ce nuclei for neutron number  $60 \leq N \leq 80$  [4], gave rise to a value of  $\beta = 0.365$  MeV, a value quite close to the value derived using nuclei with  $N = 80$  only, considering now the excitation energy of both the  $2_1^+$  and  $2_{1,\text{ms}}^+$  states. Making use of the fitted value of  $\beta = 0.35(1)$  MeV as derived in the present study and using the expression of  $\beta$  as derived from Eq. (3.4) of Ref. [4], a rather precise value of the strength  $\kappa$  of the quadrupole–quadrupole proton–neutron residual interaction can be derived using the  $50 \leq Z, N \leq 82$  mass region. A value of  $\kappa = 0.15(1)$  MeV results, considering the limit  $j \rightarrow \infty$ , which is a good approximation for the large  $j$  values  $7/2, 11/2$  that are relevant in this mass region (see Fig. 2 and Table II in Ref. [30]). This strength is very close to that derived independently in shell-model calculations of the energy spectra for odd–odd Sb and I nuclei [31].

The good agreement between the simple scheme presented here and the data (see Fig. 5) supports the concept that the evolution of the one-phonon states predominantly results from a two-state mixing between the proton and the neutron  $2^+$  excitations which itself is governed by the proton–neutron quadrupole interaction [4]. The slight deviation of the experimental energy of the  $2_{1,\text{ms}}^+$  states in  $^{138}\text{Ce}$  from the smooth evolution must be expected due to the lack of shell stabilization of MSSs at the  $\pi 1g_{7/2}$  closure [9], a mechanism which is outside the framework of the simple two-state mixing model considered here. Note however, that the energy of the  $2_1^+$  state, agrees very well with the results of the fit. The result for the relative strength of the proton–neutron quadrupole interaction (the parameter  $\beta$ ) in the  $N = 80$  isotones simultaneously accounts for the properties of both symmetric and MSSs [4]. To our knowledge, this is the first instance where the dominant interaction in the valence shell, the proton–neutron quadrupole interaction, is determined locally from data on symmetric and mixed-symmetry states.

The fit procedure and the available experimental data allows for unambiguous determination of the free parameters,  $b$  and  $\beta$  that, as discussed above, describe the evolution of the one-phonon states with increasing proton number. This allows for a prediction of the energy of the  $2_{1,\text{ms}}^+$  state of  $^{132}\text{Te}$ , where this level remains to be identified. According to the scheme applied above, the  $2_2^+$  level of  $^{132}\text{Te}$  at 1.665 MeV can be considered as a candidate for the one-phonon mixed-symmetry state. Tentatively assigned  $2^+$  states of  $^{132}\text{Te}$  are included in Fig. 5, plotted with asterisks. Experimental verification of a large  $B(M1; 2_2^+ \rightarrow 2_1^+)$  value

in  $^{132}\text{Te}$  would represent the first solid identification of a MSS in a radioactive nucleus.  $^{132}\text{Te}$  has only one proton boson and one neutron boson. Consequently, the absolute value of the proton–neutron interaction matrix element is smallest for this nucleus, resulting in a mixed-symmetry state at a lower energy than the others in this isotonic chain. Very similar results on the relative variation in excitation energy of the lowest symmetric  $2_1^+$  and mixed-symmetric  $2_{1,\text{ms}}^+$  states in light, even–even Cd nuclei, as a function of the atomic mass number, i.e.,  $^{100-106}\text{Cd}$  ( $52 \leq N \leq 58$ ) have been obtained from large-scale shell-model calculations using an effective realistic force [32]. However, experimental data on mixed-symmetric  $2^+$  states in this region are scarce [33].

In summary, a Coulomb excitation experiment in inverse kinematics was carried out to identify the  $2_{1,\text{ms}}^+$  state of  $^{134}\text{Xe}$ . Three multipole mixing ratios and nine transition strengths were measured with good accuracy. From the  $M1$  strength distribution, the  $2_3^+$  state was identified as being the dominant fragment of the  $2_{1,\text{ms}}^+$  mixed-symmetry state. Looking at the  $N = 80$  isotones, an increase in the energy splitting between the  $2_1^+$  and  $2_{1,\text{ms}}^+$  states can be seen. This separation in energy was empirically fitted using a simple two-state mixing scheme where the interaction between the two states increases in strength as  $V(N_\pi) = \beta\sqrt{N_\pi N_\nu}$ . The relative strength of the proton–neutron quadrupole interaction was derived for the first time from the properties of both, symmetric and mixed-symmetric one-phonon states. The calculations also suggest that a  $2^+$  state in  $^{132}\text{Te}$  at an excitation energy around 1.7 MeV should be the dominant fragment of the  $2_{1,\text{ms}}^+$  state. It is desirable to test this expectation in future experiments with radioactive  $^{132}\text{Te}$  beams. These results point towards the predominance of the quadrupole component in the proton–neutron interaction in order to explain the relative excitation energy of the lowest symmetric and mixed-symmetric  $2^+$  states near closed shells.

## Acknowledgements

We thank the technical staff of the ATLAS facility at Argonne National Laboratory for its work in preparing and producing the  $^{134}\text{Xe}$  beam for this experiment, C. Bauer for his assistance in calculating the statistical tensors, and F. Iachello for enlightening discussions on the interpretation of our results. G.R. acknowledges the support from the BGNSF under contract DO 02-219. This work was supported by the DFG under grant Nos. SFB 634 and Pi 393/2-1, by the Helmholtz International Center for FAIR, by the US Department of Energy, Office of Nuclear Physics, under contract No. DE-AC02-06CH11357 and No. DE-FG02-91ER40609 and is partially supported by the German–Bulgarian exchange program under grants D/06/05918 and DAAD-09. Financial support from the FWO–Vlaanderen is acknowledged. This research was also performed in the framework of the BriX network (IAP P6/23) funded by the Inter-University Attraction Poles Program, Belgian State–Belgian Science Policy.

## References

- [1] R.F. Casten, D.S. Brenner, P.E. Haustein, Phys. Rev. Lett. 58 (1987) 658.
- [2] R.B. Cakirli, R.F. Casten, Phys. Rev. Lett. 96 (2006) 132501.
- [3] F. Iachello, A. Arima, The Interacting Boson Model, in: Cambridge University Press, Cambridge, 1987.
- [4] K. Heyde, J. Sau, Phys. Rev. C 33 (1986) 1050.
- [5] A. Arima, T. Otsuka, F. Iachello, I. Talmi, Phys. Lett. B 66 (1977) 205.
- [6] T. Otsuka, A. Arima, F. Iachello, Nucl. Phys. A 309 (1978) 1.
- [7] I. Wiedenhöver, A. Gelberg, T. Otsuka, N. Pietralla, J. Gableske, A. Dewald, P. von Brentano, Phys. Rev. C 56 (1997) R2354.

- [8] N. Pietralla, D. Belic, P. von Brentano, C. Fransen, R.-D. Herzberg, U. Kneissl, H. Maser, P. Matschinsky, A. Nord, T. Otsuka, H.H. Pitz, V. Werner, I. Wiedenhöver, Phys. Rev. C 58 (1998) 796.
- [9] G. Rainovski, N. Pietralla, T. Ahn, C.J. Lister, R.V.F. Janssens, M.P. Carpenter, S. Zhu, C.J. Barton III, Phys. Rev. Lett. 96 (2006) 122501.
- [10] J.R. Vanhoy, J.M. Anthony, B.M. Haas, B.H. Benedict, B.T. Meehan, S.F. Hicks, C.M. Davoren, C.L. Lundstedt, Phys. Rev. C 52 (1995) 2387.
- [11] S.F. Hicks, C.M. Davoren, W.M. Faulkner, J.R. Vanhoy, Phys. Rev. C 57 (1998) 2264.
- [12] T.C. Li, N. Pietralla, C. Fransen, H. von Garrel, U. Kneisse, C. Kohstall, A. Linne-  
mann, H.H. Pitz, G. Rainovski, A. Richter, M. Scheck, F. Stedile, P. von Brentano,  
P. von Neumann-Cosel, V. Werner, Phys. Rev. C 71 (2005) 044318.
- [13] W.D. Hamilton, A. Irbäck, J.P. Elliott, Phys. Rev. Lett. 53 (1984) 2469.
- [14] W.J. Vermeer, C.S. Lim, R.H. Spear, Phys. Rev. C 38 (1988) 2982.
- [15] N. Pietralla, P. von Brentano, A.F. Lisetskiy, Prog. Part. Nucl. Phys. 60 (2008) 225.
- [16] I.-Y. Lee, Nucl. Phys. A 520 (1990) 641.
- [17] P. Nolan, F. Beck, D. Fossan, Annu. Rev. Nucl. Part. Sci. 45 (1994) 561.
- [18] W.F. Mueller, M.P. Carpenter, J.A. Church, D.C. Dinca, A. Gade, T. Glasmacher,  
D.T. Henderson, Z. Hu, R.V.F. Janssens, A.F. Lisetskiy, C.J. Lister, E.F. Moore,  
T.O. Pennington, B.C. Perry, I. Wiedenhöver, K.L. Yurkewicz, V.G. Zelevinsky, H.  
Zwahlen, Phys. Rev. C 73 (2006) 014316.
- [19] A.A. Sonzogni, Nucl. Data Sheets 103 (2004) 1.
- [20] T. Yamazaki, Nucl. Data 3 (1) (1967) 1.
- [21] A. Stuchbery, Nucl. Phys. A 723 (2003) 69.
- [22] K. Alder, A. Bohr, T. Huus, B. Mottelson, A. Winther, Rev. Mod. Phys. 28 (1956) 432.
- [23] H. Ower, Ph.D. thesis, Johann-Wolfgang-Goethe-Universität zu Frankfurt am  
Main, 1980.
- [24] A. Lell, Master's thesis, Universität München, 1978.
- [25] A. Winther, J. de Boer, A computer program for multiple coulomb excitation,  
in: K. Alder, A. Winther (Eds.), Coulomb Excitation, Academic Press Inc., New  
York, 1966, p. 303.
- [26] K.S. Krane, R.M. Steffen, Phys. Rev. C 2 (1970) 724.
- [27] K.S. Krane, R.M. Steffen, R.M. Wheeler, Nucl. Data Tables 11 (1973) 351.
- [28] K. Alder, A. Winther, Electromagnetic Excitation, North-Holland Publishing Co.,  
Amsterdam, 1975.
- [29] N. Lo Iudice, C. Stoyanov, D. Tarpanov, Phys. Rev. C 77 (2008) 044310.
- [30] R. Fossion, C. De Coster, J.E. Garcia-Ramos, K. Heyde, Phys. Rev. C 65 (2002) 044309.
- [31] J. Sau, K. Heyde, Phys. Rev. C 23 (1981) 2315.
- [32] N. Boelaert, N. Smirnova, K. Heyde, J. Jolie, Phys. Rev. C 75 (2007) 014316.
- [33] A. Linnemann, Ph.D. thesis, Universität zu Köln, 2005.